18

APPROVED FOR PUBLIC RELEASE, DISTRIBUTION UNLIMITED

ALEX(01)-TR-77-08

12

EXTRACTION OF LONG-PERIOD SURFACE WAVES

TECHNICAL REPORT NO. ~~8~~

VELA NETWORK EVALUATION AND AUTOMATIC PROCESSING RESEARCH

Prepared by
Stephen S. Lane

TEXAS INSTRUMENTS INCORPORATED
Equipment Group
Post Office Box 6015
Dallas, Texas 75222

Prepared for

AIR FORCE TECHNICAL APPLICATIONS CENTER
Alexandria, Virginia 22314

Sponsored by

ADVANCED RESEARCH PROJECTS AGENCY
Nuclear Monitoring Research Office
ARPA Program Code No. 7F10
ARPA Order No. 2551

8 December 1977

Acknowledgment: This research was supported by the Advanced Research Projects Agency, Nuclear Monitoring Research Office, under Project VELA-UNIFORM, and accomplished under the technical direction of the Air Force Technical Applications Center under Contract Number F08606-77-C-0004.

ALEX(01)-TR-77-08

EXTRACTION OF LONG-PERIOD SURFACE WAVES

TECHNICAL REPORT NO. 8

VELA NETWORK EVALUATION AND AUTOMATIC PROCESSING RESEARCH

Prepared by
Stephen S. Lane

TEXAS INSTRUMENTS INCORPORATED
Equipment Group
Post Office Box 6015
Dallas, Texas 75222

Prepared for

AIR FORCE TECHNICAL APPLICATIONS CENTER
Alexandria, Virginia 22314

Sponsored by

ADVANCED RESEARCH PROJECTS AGENCY
Nuclear Monitoring Research Office
ARPA Program Code No. 7F10
ARPA Order No. 2551

8 December 1977

Acknowledgment: This research was supported by the Advanced Research Projects Agency, Nuclear Monitoring Research Office, under Project VELA-UNIFORM, and accomplished under the technical direction of the Air Force Technical Applications Center under Contract Number F08606-77-C-0004.

UNCLASSIFIED

SECURITY CLASSIFICATION OF THIS PAGE (When Data Entered)

REPORT DOCUMENTATION PAGE		READ INSTRUCTIONS BEFORE COMPLETING FORM
1. REPORT NUMBER	2. GOVT ACCESSION NO.	3. RECIPIENT'S CATALOG NUMBER
4. TITLE (and Subtitle) (6) EXTRACTION OF LONG-PERIOD SURFACE WAVES.		5. TYPE OF REPORT & PERIOD COVERED (9) Technical rept.
		6. PERFORMING ORG. REPORT NUMBER (14) TI-ALEX(Ø1)-TR-77-Ø8
7. AUTHOR(s) (10) Stephen S. Lane		8. CONTRACT OR GRANT NUMBER(s) (15) FØ8606-77-C-0004, ARPA Order-2551
9. PERFORMING ORGANIZATION NAME AND ADDRESS Texas Instruments Incorporated Equipment Group Dallas, Texas 75222		10. PROGRAM ELEMENT, PROJECT, TASK AREA & WORK UNIT NUMBERS VELA T/7705/B/ETR
11. CONTROLLING OFFICE NAME AND ADDRESS Advanced Research Projects Agency Nuclear Monitoring Research Office Arlington, Virginia 22209		12. REPORT DATE (11) 8 December 1977
		13. NUMBER OF PAGES 28
14. MONITORING AGENCY NAME & ADDRESS(if different from Controlling Office) Air Force Technical Applications Center VELA Seismological Center Alexandria, Virginia 22314		15. SECURITY CLASS. (of this report) UNCLASSIFIED
		15a. DECLASSIFICATION/DOWNGRADING SCHEDULE

16. DISTRIBUTION STATEMENT (of this Report) (12) 31p.

APPROVED FOR PUBLIC RELEASE, DISTRIBUTION UNLIMITED

17. DISTRIBUTION STATEMENT (of the abstract entered in Block 20, if different from Report)

18. SUPPLEMENTARY NOTES

ARPA Order No. 2551

19. KEY WORDS (Continue on reverse side if necessary and identify by block number)

- Seismology
- Signal processing
- Wiener filter
- Three component adaptive filter
- Matched filter
- Detection threshold
- Surface waves

20. ABSTRACT (Continue on reverse side if necessary and identify by block number)

Gains from a cascaded Wiener filter, three component adaptive (TCA) filter, and prewhitened matched filter were measured for various orders of application to long-period surface waves buried in seismic noise. It was found that the gain of the cascaded Wiener filter and three component adaptive filter was greater than the sum of their individual gains, and that this was the best order of application, but that following them with the matched filter reduced the overall gain over the range of input signal to noise ratio → next page

DD FORM 1 JAN 73 1473 EDITION OF 1 NOV 65 IS OBSOLETE

UNCLASSIFIED 4B Page

SECURITY CLASSIFICATION OF THIS PAGE (When Data Entered)

405 076

20. Abstract (continued)

of interest. These results are due to the non-linear nature of the TCA and to the distortion inherent in its output.

A large number of earthquakes from the Kurile Islands as recorded at the Guam Seismic Research Observatory were processed using cascaded Wiener filter, TCA, and matched filter, in that order. The body wave magnitude at which 50% of the events were detected by means of long-period surface waves was reduced from m_b=4.6, the value when only a bandpass filter was used, to near m_b=3.8. The precise threshold using cascading could not be determined accurately due to a lack of non-detected events at low magnitudes. Use of the matched filter added no detections to those achieved by the other two processors.

Surface wave magnitudes associated with these detections decreased linearly with m_b to about m_b=4.0, where they decreased no further, due to bias from noise. Over their linear range they lay about 0.2 M_s units below the M_s-m_b relation for bandpass filtered data, implying a signal degradation of that amount.

ABSTRACT

Gains from a cascaded Wiener filter, three component adaptive (TCA) filter, and prewhitened matched filter were measured for various orders of application to long-period surface waves buried in seismic noise. It was found that the gain of the cascaded Wiener filter followed by the three component adaptive filter was greater than the sum of their individual gains, and that this was the best order of application, but that following them with the matched filter reduced the overall gain over the range of input signal-to-noise ratio of interest. These results are due to the non-linear nature of the TCA and to the distortion inherent in its output.

A large number of earthquakes from the Kurile Islands as recorded at the Guam Seismic Research Observatory were processed using cascaded Wiener filter, TCA, and matched filter, in that order. The body-wave magnitude at which 50% of the events were detected by means of long-period surface waves was reduced from $m_b = 4.6$, the value when only a band-pass filter was used, to near $m_b = 3.8$. The precise threshold using cascading could not be determined accurately due to a lack of non-detected events at low magnitudes. Use of the matched filter added no detections to those achieved by the other two processors.

Surface wave magnitudes associated with these detections decreased linearly with m_b to about $m_b = 4.0$, where they decreased no further, due to bias from noise. Over their linear range they lay about 0.2 M_s units below the $M_s - m_b$ relation for bandpass filtered data, implying a signal degradation of that amount.

ACKNOWLEDGEMENT

Helena Scott's help in processing the data used here is gratefully acknowledged.

TABLE OF CONTENTS

LIST OF FIGURES

SECTION I

INTRODUCTION

In a previous report, the performance of three seismic signal processors, as applied to long-period surface wave data, was examined. The processors were optimized in that study by burying large signals in noise at known levels, and comparing the gains achieved by each processor with that of a simple bandpass filter.

The present report extends that work to the measurement of the gains of cascaded processors; that is, the total gain when the output of one filter is used as the input of another. Also, detection threshold reduction is measured by applying the cascaded processors to observed data, and surface wave magnitudes are obtained from detections so as to examine their behavior.

Section II of this report describes the processors studied. Section III is concerned with the gain and amplitude degradation to be expected from the cascaded signal processors, and Section IV presents the threshold reduction and magnitudes measured from a large data set. Conclusions are presented in Section V.

SECTION II
SIGNAL PROCESSORS

Three seismic signal processors - a Wiener filter, a prewhitened matched filter, and the three component adaptive filter (TCA) - are studied in this report and are briefly described here. A more complete description is given by Lane (1976).

The functional form of the frequency domain Wiener filter (Robinson and Trietel, 1967) is:

$$W(\omega) = \frac{\phi_{ss}(\omega)}{\phi_{ss}(\omega) + \phi_{nn}(\omega) + \phi_{sn}(\omega) + \phi^*_{sn}(\omega)} \qquad \text{(II-1)}$$

where ϕ_{ss} is the expected value of the signal power spectrum, ϕ_{nn} the expected value of the noise power spectrum, ϕ_{sn} the expected value of the signal-noise correlation function, and ω the angular frequency. The symbol * denotes the complex conjugate.

The expected signal spectrum ϕ_s is found by averaging together amplitude and phase spectra from a number of large events from a small source region. Separate filters should be designed for earthquakes and explosions. The square of the amplitude spectrum, ϕ_{ss}, is the signal power spectrum required by equation (II-1), and is only suitable for the detection of events from the region used to form ϕ_s. The noise power spectrum is found by averaging spectra for several segments of noise prior to the signal arrival time, thus increasing the reliability of the resulting spectrum. The signal-noise correlation term ϕ_{sn} is taken to be zero, as usual.

The form of the matched filter is:

$$M(\omega) = \frac{\phi_s^*(\omega)}{\phi_{nn}(\omega)} \quad . \tag{II-2}$$

The spectra ϕ_s and ϕ_{nn} are those found by averaging as for the Wiener filter. The matched filter is again appropriate only to the region for which ϕ_s was formed.

The TCA filter segments the time data, Fourier transforms it, designs and applies a filter whose weights depend on how well the data fit a model of the signal and noise, inverse transforms, and smooths overlapping segments together to give continuous filtered data. The model for Rayleigh waves assumes that uncorrelated noise is present with equal amplitude on radial and vertical traces, and that the radial phase lags the phase of the vertical component by $\pi/2$. Weights are assigned according to how well the observed data fit this model, and applied equally to the radial and vertical traces.

The Love wave model assumes that the noise is equal and uncorrelated on the radial and transverse components, and that the signal is present on the transverse component only. High filter weights are applied to the transverse component when the data fit this model, while radial and vertical motions are unaffected. For both filters, data outside the expected signal band from 0.024 Hz to 0.059 Hz are set to zero.

Lane (1976) presents the results of processing large signals buried in seismic noise at known signal-to-noise ratio with each of these processors individually. The Wiener filter achieved gains over a simple bandpass filter of up to 6 dB. The matched filter's performance on a given signal-noise sample pair was similar to that of the Wiener filters in terms of the shape of the gain versus input level curve, but gains were about 4 dB higher. The TCA had the highest gain, amounting to 15 dB in some cases, but this was achieved at the expense of noticeable signal distortion.

SECTION III

PERFORMANCE ON SIGNALS BURIED IN NOISE

Here we present curves of gain of cascaded signal processors over bandpass filtered results, using large events buried in seismic noise at known levels. The signal degradation produced by this process is also reported.

It is clear that the matched filter should be applied last in any cascade of signal processors, since its output contains no information concerning the signal other than time of arrival and amplitude, and the TCA and Wiener filter require more information than this for implementation. Furthermore, since the TCA is a non-linear filter whose gain increases as the input signal-to-noise ratio increases, it is important to precede it with the best possible prefilter. Thus the logical processing sequence is Wiener filter followed by TCA followed by matched filter. Results will be presented here for this sequence, and these results are better than those achieved by any other combination tested.

Figure III-1 shows typical results for the radial component of a large signal buried in seismic noise. The signal in this case was generated by an event from Kamchatka on day 231 of 1976 and recorded at a single site at ALPA. The noise was recorded on day 41 of the same year. The horizontal axis is the true signal-to-noise ratio (peak signal to RMS noise) at which the event was buried, and the vertical axis is the gain of various processors over a simple bandpass filter.

The Wiener filter showed very little improvement over the bandpass filter for this signal-noise combination, never achieving more than 0.7 dB gain. When followed by the TCA, however, over 10 dB gain

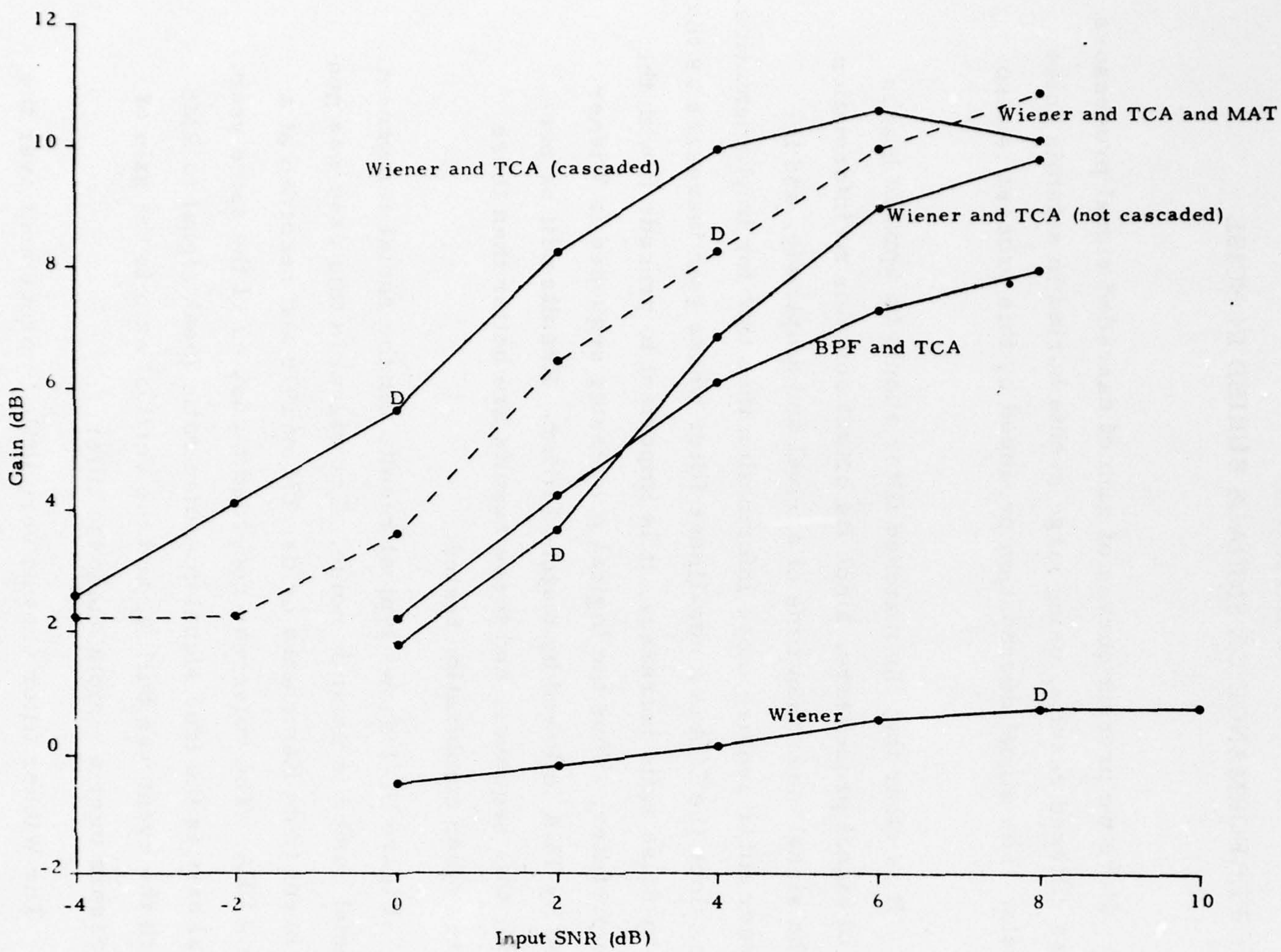

FIGURE III-1

GAIN VERSUS INPUT SIGNAL TO NOISE RATIO

was found at 6 dB input signal-to-noise ratio. When the matched filter (MAT) followed the Wiener filter and the TCA, the gain was reduced somewhat over most of the range of input signal-to-noise ratios studied.

This reduction in gain occurred for every combination of signal and noise studied, and is due to the distortion of the output signal by the TCA, as noted by Lane (1976). Only at the highest input levels are the outputs sufficiently faithful reproductions of the inputs for the matched filter to yield any gain.

Also plotted on Figure III-1 is the sum of the gains of the Wiener filter and the TCA when applied to the data separately. These gains do not sum to the gain achieved by the cascaded processors due to the non-linear nature of the TCA. It is of interest that the matched filter begins to show gain over the cascaded Wiener filter and TCA at about the same point as that where the Wiener filter and TCA gains sum to the cascaded gain. This is because at that level the TCA has become nearly linear and its output is becoming a closer replica of the input waveform.

For comparison, the gain of a cascaded bandpass filter and TCA is also shown on Figure III-1. The Wiener filter improves the performance of the TCA by about 4 dB relative to the bandpass filter, although the gain of the Wiener filter alone is negligible. This is, of course, due to the non-linear nature of the TCA.

Two effects combine to prevent the threshold reduction of cascaded detectors from being as great as implied by the gain curves of Figure III-1. These are the presence of interfering events, and variations in signal amplitude.

The Wiener filter requires an estimate of the noise power spectrum at the time of the signal arrival, and this is obtained by averaging power spectra for as many 128 point segments of noise as are available before the predicted signal arrival time. If a large event precedes the desired signal, only a few segments, or none, may be available for purposes of noise estimation, even though no interfering event energy actually appears in the signal arrival gate. A Wiener filter designed under this handicap will naturally give performance inferior to one which has a good estimate of the noise power spectrum. Since the events used in the detector evaluation occurred in large part in swarms, a significant number of them were affected. Long-period bodywaves, which are of only a few cycles duration and are undetectable in the magnitude range of interest, will not contaminate the noise power spectrum significantly.

Second, the Wiener filter also requires the expected signal power spectrum. Effectively this is a requirement for the expected signal peak amplitude. This amplitude, A, was found in the present study by eliminating M_s from the empirical relationship between M_s and m_b.

$$M_s = -2.22 + 1.25\, m_b \qquad \text{(III-1)}$$

and the definition of M_s

$$M_s = \log\left(\frac{A}{T}\right) + \log(\Delta) \qquad \text{(III-2)}$$

where Δ is the epicentral source to receiver distance, A is the peak-to-peak amplitude, and T is the period.

However, due to variations in observed surface wave magnitude about the average value at a given m_b, the amplitude predicted by equations (III-1) and (III-2) may be in error by a factor of 3 or more. This will introduce an error of unknown magnitude into the Wiener filter design, and thus into its output.

The detection threshold at which each signal was first detected is marked with the letter D on Figure III-1. Detection thresholds are much more subjective measurements than are gains, so less weight should be placed on the threshold reduction achieved. It should also be remembered that the detection with the matched filter was made without the aid of dispersion, contributing to its relatively poor performance. The point marked D for the sum of the Wiener and TCA gains is that at which the TCA alone detected. There is perhaps less reduction in threshold than implied by the increased gain of the cascaded Wiener filter - TCA. This is due to the reduced dispersion present in the cascaded output resulting from the somewhat reduced bandwidth of the Wiener filter output. Consequently, a somewhat higher signal-to-noise ratio is required for detection with the cascaded Wiener filter - TCA.

One advantage of studying detector performance by burying a signal in noise is that the correct output amplitude is exactly known, and the signal degradation introduced by the processor can be measured. When this is done for the Wiener filter described here and by Lane (1976), it was found that losses in peak amplitude of from 10 to 20 dB were usual over the range of input levels studied. This is not surprising when it is remembered that the design criterion for the Wiener filter is based on power rather than peak amplitude.

This loss is unacceptable for discrimination, so the output of the Wiener filter was multiplied by a scale factor of the form $10/(SNR)^{1.3}$, which was derived empirically by comparison of Wiener filter input and output peak amplitudes. Signal degradation for the Wiener filter, for the cascaded Wiener filter and TCA are shown in Figure III-2, for the same signal and noise combination used in Figure III-1, but not the combination used to derive the multiplicative scale factor. Wiener filter losses now range from 2 to 5 dB, while TCA losses range from 5 to 10 dB. The TCA losses are of course greatest at low input signal-to-noise ratios, where signal distortion

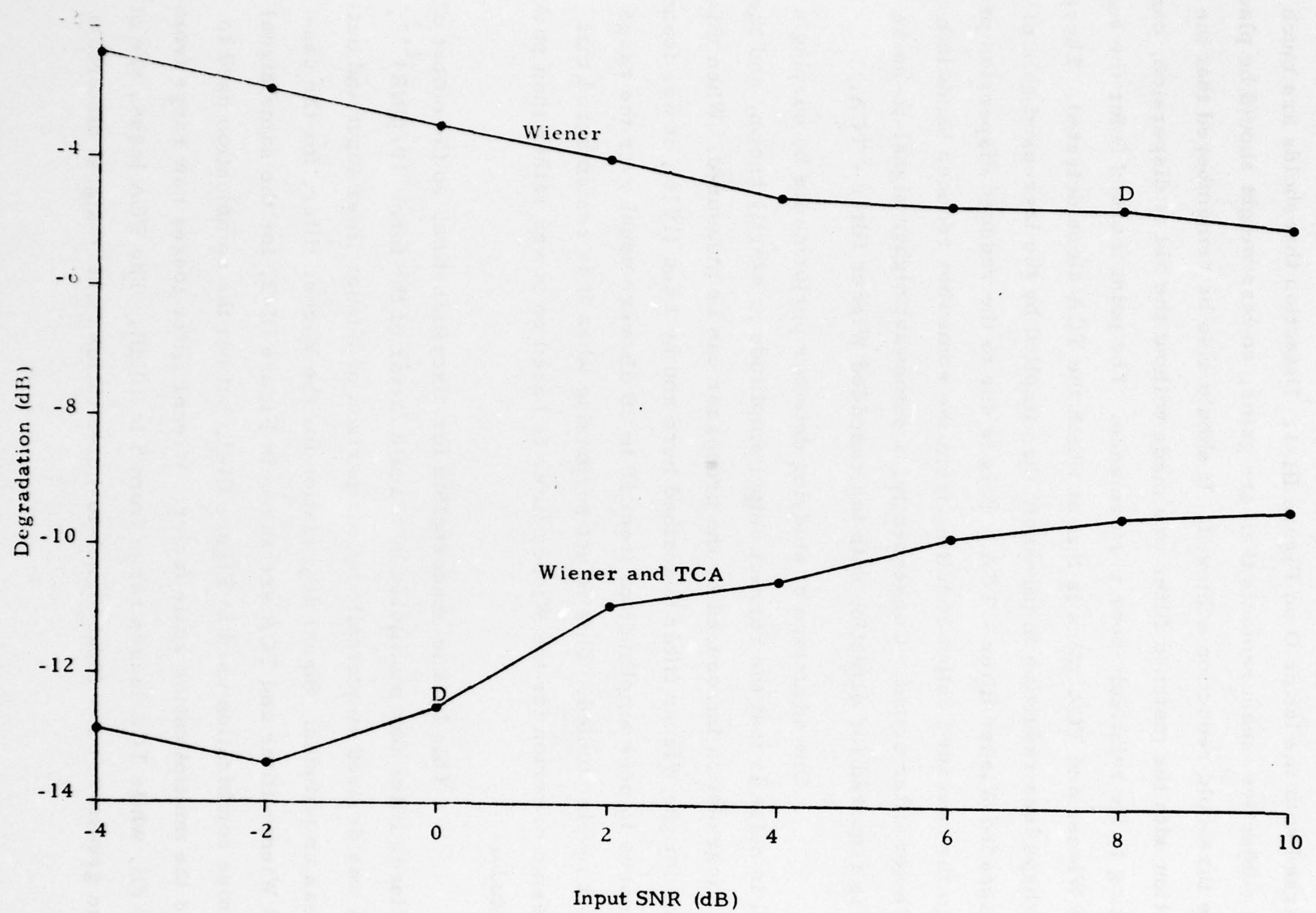

FIGURE III-2

SIGNAL DEGRADATION VERSUS INPUT SIGNAL TO NOISE RATIO is greatest. Losses claimed at inputs below detection are for the appropriate peak, even though it was not the dominant peak on the record, and may be contaminated by noise. It is encouraging that for this combination of signal and noise, at least, the net loss is relatively constant.

SECTION IV
PERFORMANCE ON RECORDED DATA

A. DETECTION THRESHOLDS

While curves of gain versus input signal-to-noise ratio are valuable for optimizing filter design and gaining insight into a filter's characteristics, the final test of performance is the filter's effect on the detection threshold. In this study of the 50% threshold, the bodywave magnitude at which we expect 50% of all events to be detected by means of their surface waves, was measured by processing 115 events from the Kurile Islands as recorded at the Guam Seismic Research Observatory. Thresholds were measured for data which had been simply bandpass filtered, and which had been processed with cascaded Wiener, TCA, and matched filters. The distribution of these events with NORSAR bodywave magnitude is shown in Figure IV-1. NORSAR magnitudes are used since they are unbiased by non-detections due to noise (Ringdal, 1975).

Figure IV-2 shows histograms of detected and non-detected events as a function of NORSAR bodywave magnitude for events processed with the bandpass filter only. Detections were claimed if waveforms met Strauss' (1977) criteria for detection. Peaks were required to be twice as large as any other peak in the preceding 600 seconds if no dispersion was present, although they could be smaller if there was dispersion.

Also in Figure IV-2 are detection probabilities as a function of magnitude and the associated fit of a cumulative Gaussian function, whose mean is the 50% detection threshold. This threshold is $m_b = 4.6$ for this data sample, a typical value for surface waves at a single station.

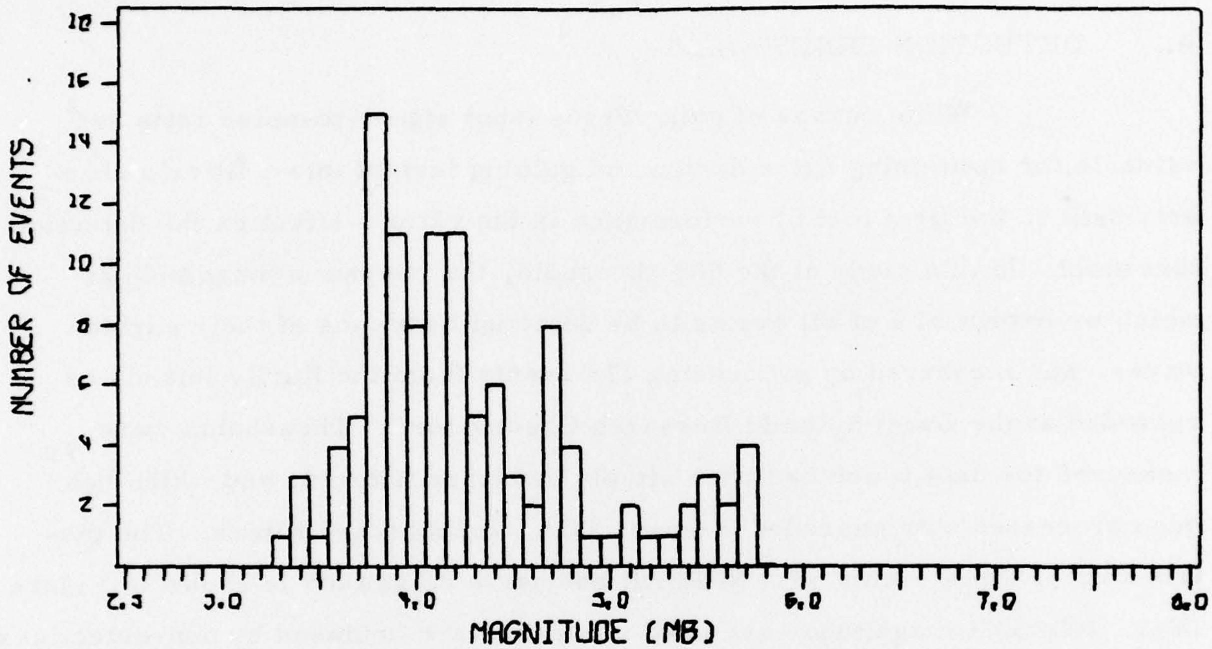

FIGURE IV-1

TOTAL EVENTS USED FOR SURFACE WAVE DETECTIONS

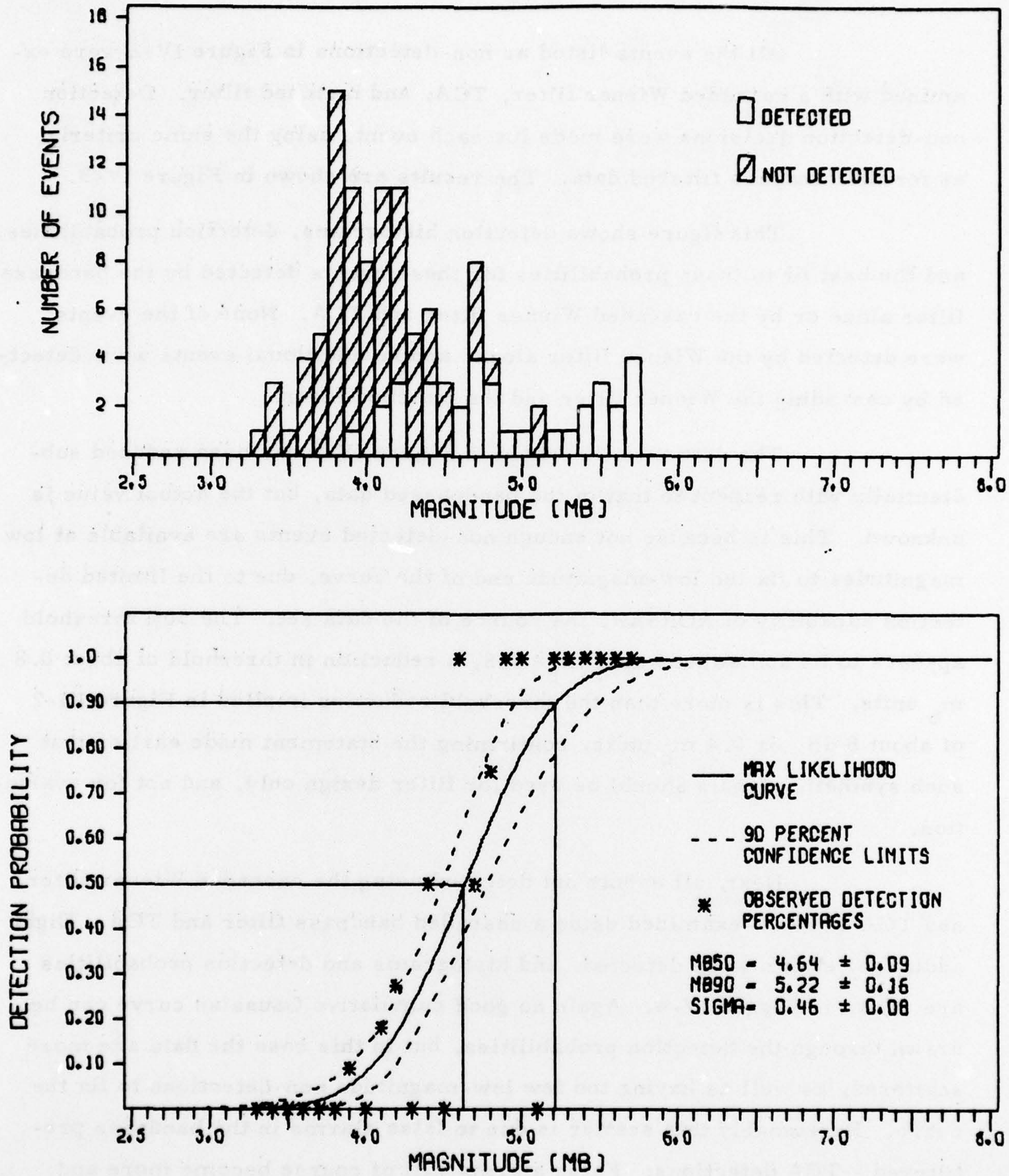

FIGURE IV-2
BANDPASS FILTER DETECTIONS

All the events listed as non-detections in Figure IV-2 were examined with a cascaded Wiener filter, TCA, and matched filter. Detection non-detection decisions were made for each event, using the same criteria as for the bandpass filtered data. The results are shown in Figure IV-3.

This figure shows detection histograms, detection probabilities, and the best fit to those probabilities for these events detected by the bandpass filter alone or by the cascaded Wiener filter and TCA. None of the events were detected by the Wiener filter alone, and no additional events were detected by cascading the Wiener filter and the matched filter.

The detection threshold in Figure IV-3 has been reduced substantially with respect to that of the bandpassed data, but the actual value is unknown. This is because not enough non-detected events are available at low magnitudes to fix the low-magnitude end of the curve, due to the limited detection capability of NORSAR, the source of the data set. The 50% threshold appears to be somewhere near $m_b = 3.8$, a reduction in threshold of about 0.8 m_b units. This is more than the threshold reduction implied in Figure III-2 of about 8 dB, or 0.4 m_b units, confirming the statement made earlier that such synthetic signals should be used for filter design only, and not for evaluation.

Next, all events not detected using the cascaded Wiener filter and TCA were re-examined using a cascaded bandpass filter and TCA. Eight additional events were detected, and histograms and detection probabilities are shown in Figure IV-4. Again no good cumulative Gaussian curve can be drawn through the detection probabilities, but in this case the data are more scattered, as well as having too few low-magnitude non-detections to fix the curve. Presumably this scatter is due to false alarms in the bandpass prefiltered - TCA detections. False alarms will of course become more and more likely as the same events are subjected to different processing schemes. Due to this scatter, no claims are made as to threshold reduction by the bandpass prefilter.

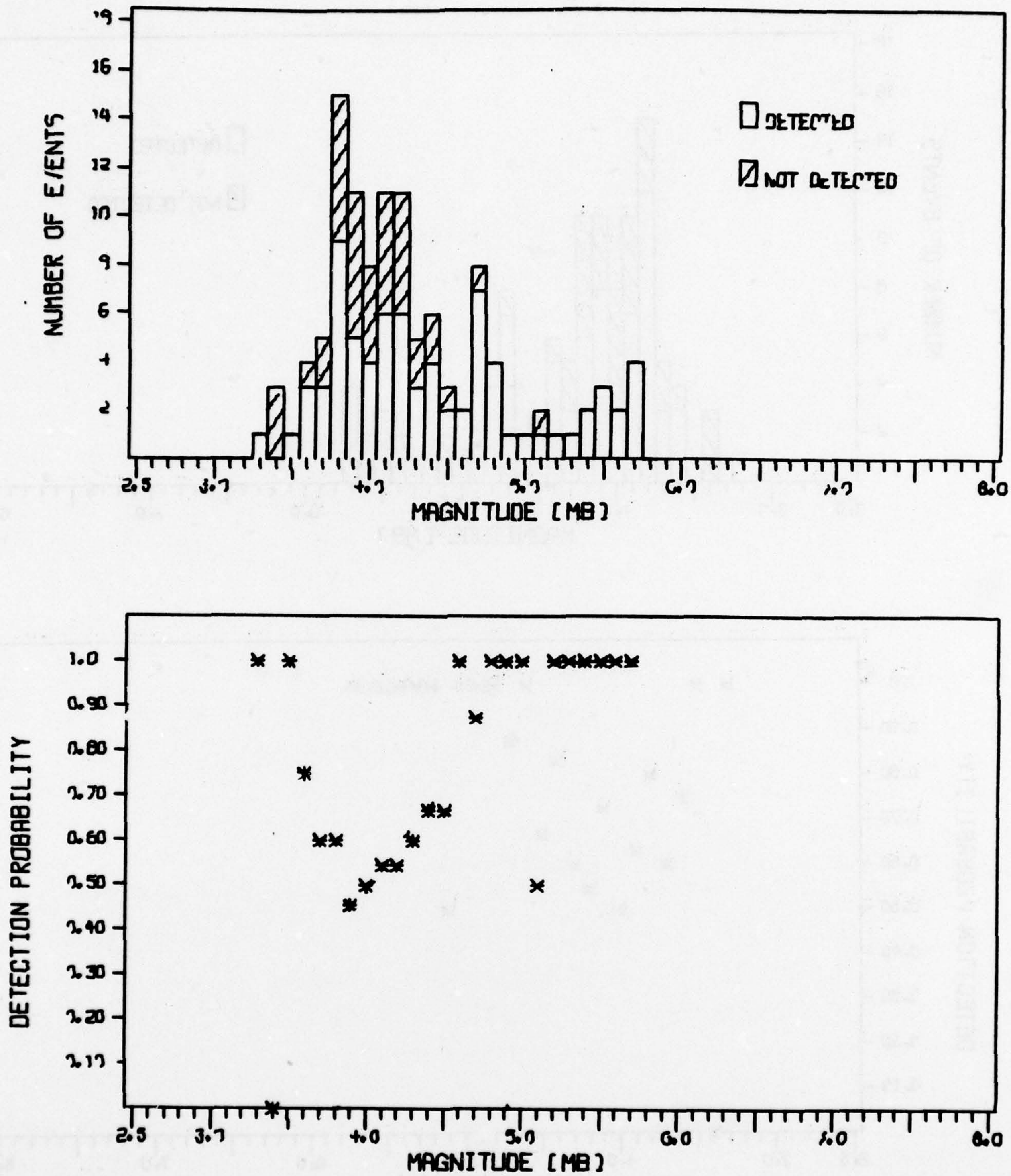

FIGURE IV-3

WIENER PREFILTER DETECTIONS

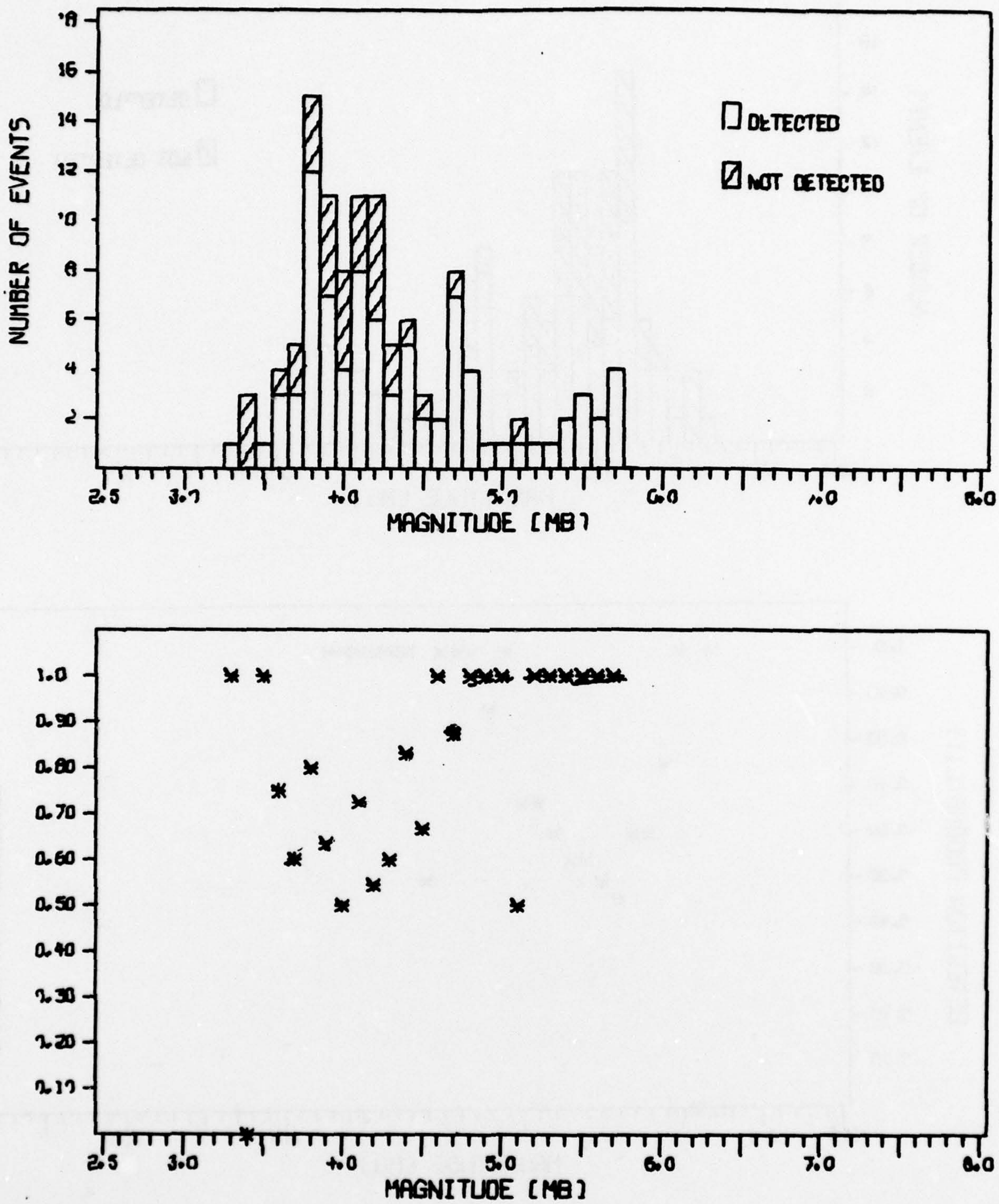

FIGURE IV-4

WIENER PREFILTER AND BANDPASS PREFILTER DETECTIONS

Considerable scatter in the detection probability at low magnitudes is present in both Figures IV-3 and IV-4. This is due to the small number of events in this region, leading to great statistical fluctuations in detection probability. Such points must be given low weight in any curve fitting procedure.

B. SURFACE WAVE MAGNITUDES

Next we consider magnitudes measured for the detections of Figure IV-3. The average surface wave magnitude at each bodywave magnitude is found by the cascaded Wiener and TCA, and by conventional bandpass filter alone, are plotted in Figure IV-5. Error bars represent one standard deviation; their absence indicates that only one event was present at that magnitude.

The best linear fit to the cascaded measurements is

$$M_s = -0.37 + 0.80\, m_b$$

with correlation coefficient 0.63. The best fit to the conventionally measured data in Figure IV-5 is

$$M_s = -1.27 + 1.09\, m_b$$

with correlation coefficient 0.81. The best fit to the set including cascaded and conventional processing is

$$M_s = -1.67 + 1.15\, m_b$$

with correlation coefficient 0.86. These curves are plotted over their range of validity on Figure IV-5.

However, linear fits to the data of Figure IV-5 are not really appropriate, although they are often quoted. Both the conventionally measured and the cascaded data suffer from bias at low magnitudes, due to the fact that only those events with relatively high M_s values are detected at low m_b's.

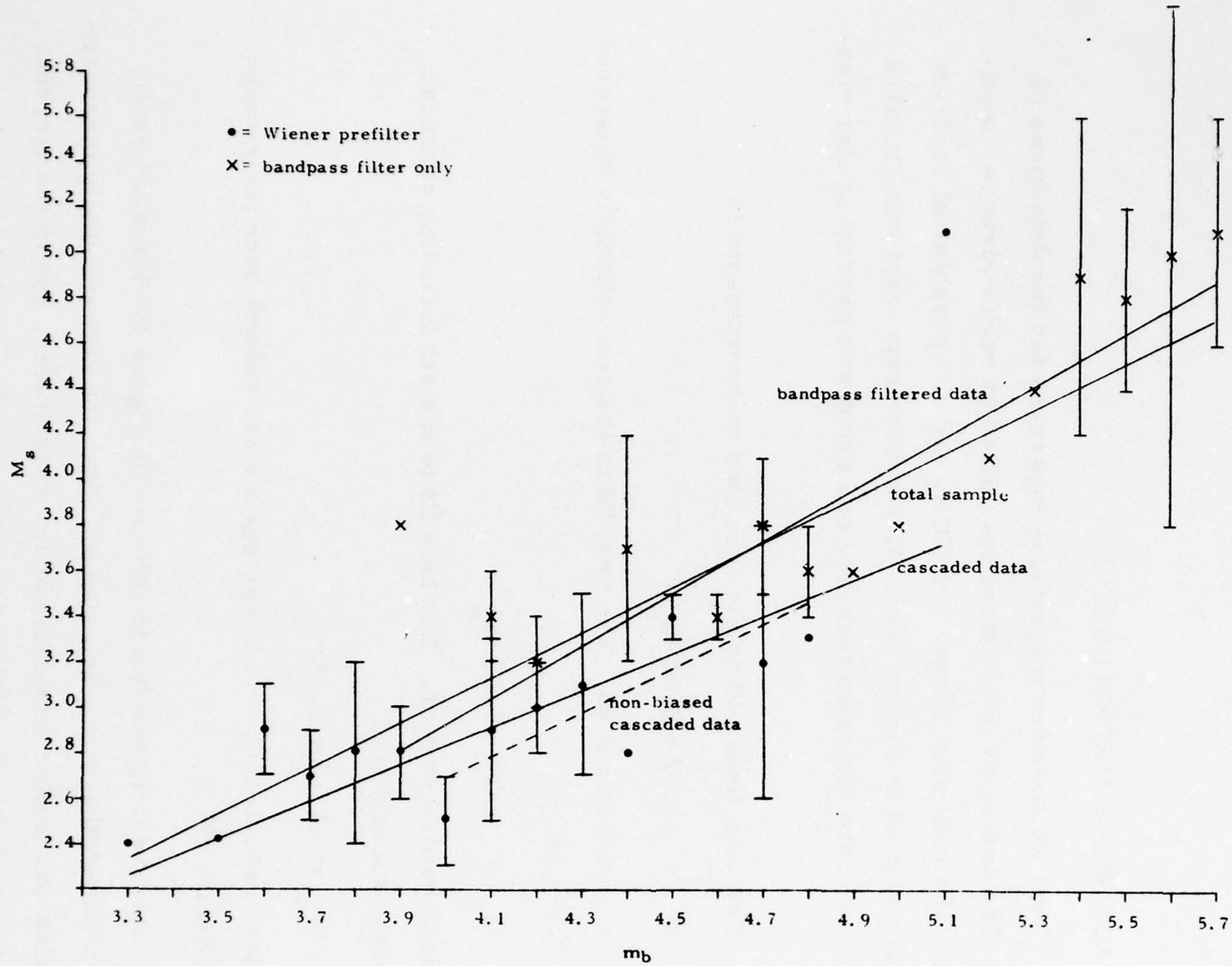

FIGURE IV-5

M_s VERSUS m_b

This effect is evidenced by a flattening of the $M_s - m_b$ relationship with respect to its behavior at higher magnitudes, and sets in at about $m_b = 4.1$ for the cascaded measurements and 4.8 for bandpass filter measurements. Assuming that the 50% detection threshold is somewhat below the break for the cascaded measurements as it is for the conventional ones, we again arrive at a threshold near $m_b = 3.8$ for the cascaded Wiener and TCA processors.

The dashed line in Figure IV-5 is a fit to the cascaded data between $m_b = 4.0$ and 5.0. It is roughly parallel to the line through the bandpass filtered results and about 0.2 to 0.3 M_s units below it. We may take this offset as the approximate degradation introduced by the cascaded processors. The magnitude of this effect is apparently less than that due to noise bias as described above. Furthermore, it is less than that of Figure IV-3, although it is nearly constant, as implied by that figure. This re-emphasizes the point that evaluations should be conducted on real rather than synthetic data.

We conclude from the similarity of the best fits through the various populations of Figure IV-5 that the data are probably all from the same population, so that magnitudes measured by the cascaded Wiener filter - TCA can be used for discrimination purposes with appropriate correction for amplitude degradation due to cascaded processing. The amplitude degradation implied by Figure IV-5 is not considered highly significant to the detection process.

SECTION V
CONCLUSIONS

The cascaded Wiener filter and TCA examined here show greater gain than would be predicted by summing their individual gains when applied to synthetic signals, whereas cascading then with a matched filter lead to a reduction in gain. When applied to real signals the bodywave magnitude at which half the events could be detected by long-period surface waves was reduced by about 0.8 m_b units. The matched filter showed no further improvement in threshold, as was expected.

Signal degradation when the cascaded Wiener filter and TCA were applied to the data set used here was estimated at about 0.2 m_b units, but was not considered highly significant when compared to other sources of bias inherent in magnitude estimation.

To establish more realistic estimates of the detection and measurement gains to be obtained by using the processor, and to establish the optimum procedure for using it in a network setting additional study is needed. Specifically, a large number of events of m_b 4.0 should be processed to fix the low m_b end of the detection curve.

SECTION VI
REFERENCES

Lane, S. S., 1976; Development of Three Signal Processing Techniques, Technical Report No. 6, Texas Instruments Report No. ALEX(01)-TR-76-06, AFTAC Contract Number F08606-76-C-0011, Texas Instruments Incorporated, Dallas, Texas.

Ringdal, F., 1975; Maximum Likelihood Estimation of Seismic Event Magnitude from Network Data, Technical Report No. 1, Texas Instruments Report No. ALEX(01)-TR-75-01, AFTAC Contract Number F08606-75-C-0029, Texas Instruments Incorporated, Dallas, Texas.

Robinson, E. A., and S. Treitel, 1967; Principles of Digital Wiener Filtering, Pan American Petroleum Corporation, Tulsa, Oklahoma.

Strauss, A. C., and L. C. Weltman, 1977; Continuation of the Seismic Research Observatories Evaluation, Technical Report No. 2, Texas Instruments Report No. ALEX(01)-TR-77-02, AFTAC Contract Number F08606-77-C-0004, Texas Instruments Incorporated, Dallas, Texas.